agriculture

MDPI

*Article*

# Understanding the Impact of Liquid Organic Fertilisation and Associated Application Techniques on $N_2$, $N_2O$ and $CO_2$ Fluxes from Agricultural Soils

**Balázs Grosz [1,*], Björn Kemmann [1], Stefan Burkart [1], Søren O. Petersen [2] and Reinhard Well [1]**

[1] Thünen Institute of Climate-Smart Agriculture, 38116 Braunschweig, Germany; bjoern.kemmann@thuenen.de (B.K.); stefan.burkart@thuenen.de (S.B.); reinhard.well@thuenen.de (R.W.)
[2] Department of Agroecology, Aarhus University, Blichers Allé 20, 8830 Tjele, Denmark; sop@agro.au.dk
* Correspondence: balazs.grosz@thuenen.de

**Abstract:** The prediction of liquid manure effects on N transformations in soils and the associated $N_2O$ and $N_2$ fluxes is poor because previous investigations have mostly excluded $N_2$. The objectives of this study were thus to quantify $N_2$, $N_2O$ and $CO_2$ fluxes, the source processes of $N_2O$, $N_2O$ reduction and the depth distribution of moisture, $NO_3^-$, $NH_4^+$, water-extractable organic carbon concentration and pH in a laboratory incubation study with sandy arable soil using $^{15}N$ tracing to quantify N processes and gaseous fluxes. The soil was amended with and without artificial slurry in various manure treatments (control, surface and injected) and incubated for 10 days at varying moisture levels, where the depth distribution of control parameters was determined twice during the experiment. Manure application was found to increase $N_2$ and $N_2O$ fluxes from denitrification, with the highest fluxes occurring in the wet manure injection treatment ($33 \pm 32$ mg N $m^{-2}$ $d^{-1}$ and $36.1 \pm 39.1$ mg N $m^{-2}$ $d^{-1}$, respectively), confirming that manure injection under wet conditions enhances denitrification and possibly also $N_2O$ fluxes. This study concluded that the current dataset is suitable as a first step towards improving the capability of biogeochemical models to predict manure application effects, but further studies with more soils and refined experiments are needed.

**Keywords:** manure; hot-spot; denitrification; incubation; $^{15}N$



**Citation:** Grosz, B.; Kemmann, B.; Burkart, S.; Petersen, S.O.; Well, R. Understanding the Impact of Liquid Organic Fertilisation and Associated Application Techniques on $N_2$, $N_2O$ and $CO_2$ Fluxes from Agricultural Soils. *Agriculture* **2022**, *12*, 692. https://doi.org/10.3390/agriculture12050692

Academic Editor: Catherine Hénault

Received: 16 March 2022
Accepted: 11 May 2022
Published: 13 May 2022



## 1. Introduction

The world's growing population is increasing its demand for agricultural products, making it necessary to increase crop production, which in turn accelerates nitrogen (N) fertiliser consumption [1]. Moreover, current diets with an increasing global share of animal products is leading to a rise in livestock numbers [2,3], resulting in the need to optimise manure fertilisation with respect to nutrient efficiency and its environmental impact [4]. However, the application of organic fertilisers poses a high risk for the environment due to considerable N losses [5].

Losses of applied N as emissions of gaseous N species, such as ammonia ($NH_3$), nitric oxide (NO) and nitrous oxide ($N_2O$), contribute to air pollution, global warming and the acidification of unmanaged land and water [5]. Nitrate ($NO_3^-$), and in coarse-textured sand soils, ammonium ($NH_4^+$) leaching and gaseous N losses impair crop yields and N use efficiency (NUE); $NO_3^-$ and $NH_4^+$ also contribute to eutrophication and $NO_3^-$ causes the contamination of drinking water resources [5,6].

Nitrous oxide is a greenhouse gas and a stratospheric ozone-depleting substance [7]. Most of the $N_2O$ that is derived from agricultural activity is emitted from soils. The magnitude of these $N_2O$ fluxes is related to N management, consisting of the application and incorporation of mineral and organic fertilisers, as well as crop residues [8–10].

Nitrous oxide is mainly produced by the microbial processes of nitrification and denitrification. Its magnitude depends on the available N substrates ($NH_4^+$ and $NO_3^-$)

and the abundance of decomposable soil organic matter [11–19]. Further controls include pH [19–22], temperature [19,23], oxygen ($O_2$) concentration in the pore space [19,24] and soil gas diffusivity [25]. Aerobic conditions favour nitrification and inhibit denitrification, whereas anaerobic conditions support denitrification and inhibit nitrification. Since $N_2O$ is an intermediate product of denitrification and its reduction to $N_2$ is the final reaction step, $N_2O$ fluxes and the $N_2O/(N_2 + N_2O)$ product ratio ($N_2Oi$) are regulated via the reduction of $N_2O$ to $N_2$.

The application of organic fertilisers is controlled by rules and legislation to minimise the potential negative effects of the excessive use of organic fertilisers. This legislation regulates the application rates of nutrients (N) per unit area, the application time and the application technique [26]. Efficient application techniques, such as band application, slot injection or incorporation by tillage, are used to reduce $NH_3$ losses and $N_2O$ fluxes and improve NUE [4]. However, the exact placement of the organic fertilisers encourages the occurrence of local $O_2$ depletion due to the respiration of labile organic C, and the high concentration of $NO_3^-$ from the previous nitrification of manure-derived $NH_4^+$ may lead to a higher $N_2O$ flux from nitrification [27] and enhanced denitrification [28].

Manure application in agricultural soil thus increases $N_2O$, and $N_2$ fluxes may lead to higher fertiliser-related $N_2O$ fluxes and lower nitrogen use efficiency (NUE) compared with mineral N fertilisation [7]. Manure application on agricultural fields affects nitrification and denitrification processes via the contemporaneous transport of mineralisable organic N and mineral N, as well as labile organic carbon (C), causing $O_2$ consumption during its respiratory decomposition [19,29–31]. In the boundary zone between manure and bulk soil, this potentially leads to the local co-occurrence of anoxia and a high $NO_3^-$ concentration from the nitrification of manure-derived $NH_4^+$. The water retention of manures causes an increase in the water content of manure clumps [32]. These factors can lead to high denitrification rates [33], possibly with highly variable $N_2Oi$, because the reduction of $N_2O$ might be inhibited by low pH due to acidification by the previous nitrification of manure-derived $NH_4^+$ and a locally high $NO_3^-$ concentration.

Liquid organic fertilisers, such as cattle and pig manure slurries, and also biogas digestates in Germany, are important organic fertilisers, especially in areas with high livestock density [34]. Approximately half of the N content is in an organic form and the other half in a mineral (mostly $NH_4^+$) form. The different techniques of slurry application greatly influence gaseous N losses [33,35]. While the impact of liquid organic fertiliser incorporation techniques on $N_2O$ fluxes has been studied [33,35], only a few studies have investigated the effects of these applications on $N_2$ fluxes [36,37]. To date, there is little experimental basis for predicting how soil texture, soil and manure moisture, pH and the dynamics of organic C and mineral N interact with slurry. This will be complex, based both on the spatial distribution of the slurry and the varying properties of the slurry itself. Biogeochemical models have been widely used to predict soil $N_2O$ fluxes, for example, but the validation of the modelled denitrification rates via the direct measurement of gaseous products, including $N_2$, are generally lacking [15,38]. Until now, there has been little attempt to include the process dynamics following amendment with organic fertilisers [39–41]. Nevertheless, there are several missing but important variables and processes that are not included in the current models, such as spatial manure distribution, hotspot or pH effects and manure quality. Process-based models mostly homogenise the N, C and water content of the manure with the N and C pools and the water content of the soil [39], and this simplified process description of manure application may lead to inaccurate model simulations. Therefore, the further development and improvement of models is necessary, but this cannot be conducted without suitable measured data. One objective of the present study was to create a dataset that would be suitable for testing and developing new biogeochemical model approaches to describe manure–soil interactions.

Furthermore, this study addressed the general question of how liquid manure fertilisation and its application methods impact upon $N_2$, $N_2O$ and $CO_2$ fluxes from agricultural soils, and how this is related to the spatial distribution of control variables.

The objectives of this study were thus to quantify $N_2$, $N_2O$ and $CO_2$ fluxes and pathways of $N_2O$ production, $N_2O$ reduction and the depth distribution of moisture, $NO_3^-$, $NH_4^+$, water-extractable organic carbon (WEOC) concentration and pH, and to determine the hotspot effect of manure on the product ratio. It was hypothesised that the manure-induced boundary effect (i) increases the pH, WEOC and water content locally, (ii) increases the concentration of $NO_3^-$ due to gross N mineralisation and nitrification, and as a joint effect of these variables, (iii) increases the denitrification activity and (iv) results in a decreased $N_2O/(N_2 + N_2O)$ product ratio of denitrification in the soil surrounding the manure. Finally, it was hypothesised that (v) manure injection leads to higher rates and a lower product ratio of denitrification than does surface application.

## 2. Materials and Methods

### *2.1. Soil Selection, Ampling and Preparation*

Soil was collected in August 2016 from a sandy arable soil (referred to below as sandy soil) located near Fuhrberg, Lower Saxony, in Germany (52°33.17622′ N, 9°50.85816′ E, 40 m asl). The site is in the transition zone of the temperate oceanic climate and warm-summer humid continental climate, with a mean annual temperature of 8.2 °C and an average yearly precipitation of 680 mm. Typical crops during the preceding decades have been winter cereals (for instance, *Triticum aestivum* or *Hordeum vulgare*), potatoes, sugar beet (*Beta vulgaris*) and maize (*Zea mays*). The soil is a Gleyic Podzol [42] developed in glacifluvial sand [43,44]. The first 5 cm of soil contained incorporated winter wheat straw residues. To avoid inaccuracies in the measurement of soil parameters (Table 1), this 5 cm layer was removed by hand across a 100 $m^2$ area, followed by soil collection from a depth of 5 to 20 cm. After field collection with spades and shovels, the soil was transported to the laboratory, air dried, sieved to 10 mm, homogenised and stored in plastic boxes at 4 °C until use. The soil samples for the laboratory analyses were sieved to 2 mm. To exclude the phase of intensive respiration and mineralisation typically following rewetting, soils were pre-incubated at 35% of maximum water-holding capacity for two weeks at room temperature.

**Table 1.** Physical and chemical data of surface soil from Fuhrberg, Germany (sand, 5 to 20 cm depth).

| Clay | Silt | Sand | Bulk Density | pH ($CaCl_2$) | Total N | Organic C | C/N Ratio |
|---|---|---|---|---|---|---|---|
| [%] | [%] | [%] | [g $cm^{-3}$] | | [%] | [%] | |
| 3.1 | 5.9 | 91.0 | 1.5 | 4.82 | 0.14 | 2.1 | 15.5 |

### *2.2. Laboratory Incubation*

#### 2.2.1. Experimental Design and Incubation Set-Up

The N content of the pre-incubated soil was 33.1 mg $NO_3$-N $kg^{-1}$ dry soil and 0.9 mg $NH_4$-N $kg^{-1}$ dry soil. A $^{15}$N-labelled $KNO_3$ (98 atom% $^{15}$N) solution (69.3 mg N $kg^{-1}$ dry soil) was added after pre-incubation to the soil, and thoroughly mixed with additional water to reach the target water content of the drier treatment and the 65 atom% $^{15}$N enrichment.

The pre-incubated soil was placed in aluminium columns (9.4 cm inner diameter and 10 cm height) at bulk density (BD) according to typical field conditions (1.5 g $cm^{-3}$), and these columns were put in gas-tight Plexiglas® cylinders (14.4 cm inner diameter and 18 cm height) for the gas flux measurements. Bulk density was established by filling 1040.97 g soil in the 694 $cm^3$ aluminium column and compacting it in one step with a lever press machine as one layer. For the injected treatments, the soil was compacted in two layers.

Two soil moisture levels were established, with the target water content being expressed as a water-filled pore space (WFPS), defined here as the volumetric water content excluding the water that was added with the manure. Hence, the effective water content of the manure treatments was higher than the defined WFPS level.

Six replicates of each of the six treatments were packed (control, 40% WFPS (C40); control, 60% WFPS (C60); surface manure treatment, 40% WFPS (S40); surface manure treatment, 60% WFPS (S60); and injected manure treatment, 40% WFPS (I40); and injected manure treatment, 60% WFPS (I60)).

The temperature (15 °C) and the moisture were kept constant throughout the 10-day experiment. The WFPS of the soil after packing was 40% (equivalent to 11.6 g $g^{-1}$), which is the soil moisture level of the dry treatment. To achieve the target moisture of the wet treatments of 60% WFPS (equivalent to 17.4 g $g^{-1}$), extra water was added after the columns were filled, but before surface manure application. This therefore helped to avoid the soil being wetted before being filled in the cylinders, because a low structure stability at high moisture would have impeded homogenous packing.

Three different manure treatments were applied: control (no manure), surface (manure added to the top of the soil) and injected. For both manure treatments, the soil was almost completely covered with a layer of manure, but it was left free of manure along the edge (approximately 1 mm) of the soil to avoid the soil–air gas exchange being blocked. The injected manure layer was added to the middle (5 cm depth) of the soil column. The applied amount of the manure was equivalent to 20.8 t $ha^{-1}$ (Table S1). The added manure mixture roughly doubled the water content of the manure-amended soil layers, because 13.4 g water was added with to manure to the water content of the 1 cm soil layer, while 12.1 g of water at 40% WFPS and 18.1 g of water at 60% WFPS were present in the soil layers without manure.

The soil cylinders were incubated for 10 days, and the headspace was continuously flushed with an artificial gas mixture (2% $N_2$, 20% $O_2$, 320 ppb $N_2O$ and 300 ppm $CO_2$ in He, headspace volume: 2146.1 $cm^3$) at a flow rate of 10 mL $min^{-1}$. $CO_2$ and $N_2O$ were added to the gas mixture to mimic the assumed atmospheric levels. The low $N_2$ concentration was adopted to improve the sensitivity of the isotope ratio mass spectrometry (IRMS) measurements [45].

#### 2.2.2. Gas and Stable Isotope Analysis

The cylinders were incubated using an automated incubation system, including gas analysis by a gas chromatograph (GC, 2014; Shimadzu, Duisburg, Germany), with an electron capture detector (ECD), a flame ionisation detector (FID) and a thermal conductivity detector (TCD). After soil packing, the data points of $CO_2$ and $N_2O_T$ in the first 18 h were omitted from the analyses. Using the GC, $N_2O$ (total $N_2O$: $N_2O_T$), $CH_4$, $N_2$ and $CO_2$ concentrations were continuously measured in the outflow throughout the incubation [46,47]. Gas samples were also collected manually at days 1, 5 and 9 in 12 mL Exetainers with rubber septa (Labco Ltd., Lampeter, UK) for IRMS (MAT 253, Thermo Scientific, Bremen, Germany) analysis, to determine the fluxes of $N_2$ (fp_$N_2$) and $N_2O$ (fp_$N_2O$) originating from the $^{15}N$-labelled $NO_3^-$ [48,49] (see the Supplementary Material for the calculation). Gas sampling was accomplished by connecting two 12 mL Exetainers to the outlet flow of the columns [50]. Before disconnecting the samples, the Exetainer volume was exchanged approximately 1200 times. Nitrous oxide from other sources was calculated from $N_2O_T$ and fp_$N_2O$ ($N_2O_{os}$ = $N_2O_T$ − fp_$N_2O$). For an analytical online preparation of the sample before measurement, the samples were treated using a modified GasBench II (Thermo Scientific, Bremen, Germany). The $N_2O$ in the gas samples was reduced to $N_2$ by a hot copper wire (650 °C) in an oven located in the gas line between the GasBench II and IRMS [51]. The $^{29}R$ ($^{29}N_2/^{28}N_2$) and $^{30}R$ ($^{30}N_2/^{28}N_2$) $N_2$ isotope ratios were determined for $N_2$, $N_2$ + $N_2O$ and $N_2O$ in the gas samples.

#### 2.2.3. Slurry Preparation and Addition

After filling the cylinders with soil, 13.9 g $kg^{-1}$ artificial manure mixture (Table S1) equivalent to 85.7 kg N $ha^{-1}$ (equivalent to 57.1 mg N $kg^{-1}$, comprising 38.6 mg $NH_4^+$-N $kg^{-1}$), was added to each soil core. To supply artificial manure with a defined composition, 2.43 kg solid dairy cow faeces (Table S1) were mixed with a solution of 1.37 kg organic

material (urea: 17.117 g $dm^{-3}$, hippuric acid: 4.095 g $dm^{-3}$, allantoin: 4.744 g $dm^{-3}$, uric acid: 0.330 g $dm^{-3}$, creatinine: 1.131 g $dm^{-3}$ and altogether, 4.76 g N $dm^{-3}$), inorganic salts ($KHCO_3$: 14.0 g $dm^{-3}$, KCl: 10.5 g $dm^{-3}$, $CaCL_2$*$H_2O$: 0.4 g $dm^{-3}$, $MgCl_2$*$5H_2O$: 1.2 g $dm^{-3}$, $Na_2SO_4$: 3.7 g $dm^{-3}$) and 1.203 L water [52]. The fresh faeces were collected from dairy cows whose diet consisted of a total mixed ration containing grass silage and concentrates. The faeces were frozen at −18 °C after sampling. The solid dairy cow faeces and salt solution mixtures were matured at room temperature for 30 days to mimic manure storage practice, and then stored at −18 °C until application (Table S1).

To mimic the surface application and injection of manure, the manure was placed as one layer at a 5 cm soil depth. This differs from the slot injection geometry during field application of manure because the results of the experiment were to be used for the calibration and development of biogeochemical models. Therefore, manure placement was designed for the use of 1D models (i.e., DNDC, DailyDayCent, Coupmodel and DeNi). It should be noted that when investigating the soil–manure boundary layer, the contact area between manure and soil is more important than the actual slot injection geometry.

#### 2.2.4. Soil Analysis

Destructive soil sampling was conducted after 5 and 10 days. Three of the six replicates were removed after 5 days' incubation, and the soil columns were sliced into layers (Table 2). This was repeated after 10 days with the remaining three samples per treatment. Soil samples were analysed for $NO_3^-$, $NH_4^+$, pH ($CaCl_2$), $^{15}N$-$NO_3^-$ (frozen soil samples), WEOC [53] and water content (fresh soil samples).

**Table 2.** Soil layer of destructive sampling.

| | Control | Surface | Injected |
|---|---|---|---|
| **Number of Layers** | **1** | **4** | **7** |
| 1 | 0–10 cm | 0–1 cm | 0–2.5 cm |
| 2 | | 1–2 cm | 2.5–3.5 cm |
| 3 | | 2–3 cm | 3.5–4.5 cm |
| 4 | | 3–10 cm | 4.5–5.5 cm |
| 5 | | | 5.5–6.5 cm |
| 6 | | | 6.5–7.5 cm |
| 7 | | | 7.5–10 cm |

To determine the water content, 15 g samples were collected from each soil layer in aluminium containers and dried for 48 h at 105 °C. The gravimetric water content was calculated as the difference between the initial weight and the dry weight of the soil samples.

To analyse the $NO_3^-$ and $NH_4^+$ content, 50 g soil samples were extracted from each soil layer with 200 mL of 2 mol $dm^{-3}$ KCl solution. After one hour of shaking, the solution was filtered (MN $614\frac{1}{4}$ filters, Macherey & Nagel GmbH & Co. KG, Düren, Germany) and stored at −18 °C until concentration analyses were conducted using the colorimetric measurement method (SA 5000 continuous flow analyser, Skalar Analytical B.V., Breda, The Netherlands).

To allow the determination of the gross nitrification rate (GNR) [54], the $^{15}N$ enrichment of the soil $NO_3^-$ in each soil layer was measured using the Spin-MIRMS measurement method [55].

Soil pH was measured with a pH meter (FE20, Mettler Toledo, Urdorf, Switzerland). As sample preparation, 0.01 mol $dm^{-3}$ $CaCl_2$ solution was added to the soil and shaken for one hour.

To analyse the WEOC content of the soil layers, 5 g dry soil equivalent and 10 mL pure water were placed into a 50 mL centrifuge tube. After one minute of gently shaking by hand, the tube was placed in a centrifuge (12,000× *g* for 10 min). The supernatant was filtered through a 0.45-micron syringe filter with a vacuum system. The samples

were analysed by a TOC analyser (Dimatoc 2000, DIMATEC Analysentechnik GmbH, Essen, Germany).

The relative soil–gas diffusivity was calculated based on the approach of Moldrup et al. (2013) [56]. For the calculation, the following equation was used:

$$D_p/D_o = P\ \varepsilon^X\ (\varepsilon/\Phi)^{T_a} \quad (1)$$

$D_p$: Gas diffusion coefficient in soil ($cm^3$ air $cm^{-1}$ soil $s^{-1}$)
$D_o$: Gas diffusion coefficient in free air ($cm^2$ air $s^{-1}$)
$\varepsilon$: Soil–air content ($cm^3$ soil-air $cm^{-3}$ soil)
$\Phi$: Total porosity ($cm^3$ soil pore space $cm^{-3}$ soil)
P (model parameter): 1
X (model parameter): $1 + C_m\Phi$
$T_a$ (model parameter): 1
$C_m$ (media complexity factor): In the case of repacked soil, the value of $C_m$ was 1.

### *2.3. Statistics*

Statistical calculations were performed using the Python 3 (version: 3.8) [57] and R (version: 4.1.1) [58] programming languages. The normality of the data was tested with a Quantile–Quantile plot (Q–Q plot). To handle variance heterogeneity, cumulative $N_2O_T$, fp_$N_2$ and fp_$N_2O$ were log10 transformed. Cumulative emissions and mean core soil mineral nitrogen were tested with a one-way analysis of variance (ANOVA) on days 5 and 10. A multiple comparison of means (Tukey HSD $p < 0.05$) was performed on the $CO_2$, $N_2O_T$, fp_$N_2$, fp_$N_2O$, $NO_3^-$, $NH_4^+$, WEOC and pH data.

## 3. Results

### *3.1. Mineral N*

#### 3.1.1. Spatial and Temporal Changes in $NO_3^-$ Concentration

N from nitrate in the 0 to 10 cm layer of the C40 treatment remained close to the initial content of 104 mg N $kg^{-1}$ throughout the experiment, while C60 exhibited a slight increase of up to 8.38% until day 10 (Figure S1, Table 3).

**Table 3.** Measured average values of $NO_3^-$, $NH_4^+$, WEOC, $^{15}NO_3^-$ and pH of the entire soil columns after 10 days' laboratory incubation of sandy soil with (surface and injected) and without manure application at two WFPS (40% and 60%) levels. Averages and standard deviations of three replicate cores without (C40 and C60) manure, and with surface-applied manure (S40 and S60) and injected manure (I40 and I60) are shown. Superscript letters indicate significant differences between treatments ($p < 0.05$; Tukey HSD, n = 3).

| | $NO_3^-$ [kg N $ha^{-1}$] | $NH_4^+$ [kg N $ha^{-1}$] | WEOC [kg C $ha^{-1}$] | Isotopic Enrichment of $NO_3^-$ [atom% $^{15}N$] | pH ($CaCl_2$) |
|---|---|---|---|---|---|
| C40 | 156 ± 3.92 $^{ab}$ | 0.936 ± 0.039 $^{a}$ | 6.60 ± 0.0675 $^{a}$ | 65.9 | 4.80 ± 0.103 $^{bc}$ |
| C60 | 168 ± 19.7 $^{ab}$ | 0.878 ± 0.152 $^{a}$ | 7.65 ± 1.33 $^{a}$ | 65.1 | 4.71 ± 0.132 $^{c}$ |
| S40 | 168 ± 7.07 $^{ab}$ | 92.7 ± 106 $^{b}$ | 13.9 ± 12.2 $^{b}$ | 57.7 ± 5.18 | 5.07 ± 0.637 $^{ab}$ |
| S60 | 128 ± 35.6 $^{c}$ | 90.9 ± 95.0 $^{b}$ | 23.9 ± 26.3 $^{c}$ | 49.4 ± 9.66 | 5.10 ± 0.527 $^{a}$ |
| I40 | 177 ± 14.2 $^{a}$ | 59.4 ± 58.8 $^{c}$ | 10.46 ± 5.10 $^{b}$ | 58.0 ± 3.83 | 4.95 ± 0.355 $^{abc}$ |
| I60 | 145 ± 27.8 $^{bc}$ | 51.8 ± 49.3 $^{c}$ | 11.69 ± 6.15 $^{b}$ | 58.5 ± 2.97 | 5.00 ± 0.473 $^{ab}$ |

A significant depletion of $NO_3^-$ occurred in the S40 treatment in the first layer containing the manure, and to a lesser extent, also in the second layer, while the deeper layers, 3 and 4, tended to have higher $NO_3^-$ contents until day 5. At day 10, the $NO_3^-$ contents almost resumed their initial values in all layers (Figure S1).

A similar dynamic was evident in S60, but depletion at day 5 in the upper layers was more pronounced and also included layer 3, while the deepest layer showed values that were higher than the initial values. Between day 5 and day 10, all of the layers except

layer 4 showed clear increasing values. The values of the first and second layers increased by 470% and 131% between day 5 and day 10.

In I40, the central layer 4 containing the manure was initially lower until day 5, but it subsequently showed an increase of 40% until day 10. The adjacent layers above (3) and below (5) exhibited a similar trend, but the changes were less pronounced. Layers further away from the manure layer (1, 2, 6 and 7) showed slightly increasing tendencies during the incubation.

The $NO_3^-$ content in the central layer 4 and adjacent layer 5 of the I60 treatment was close to the initial values throughout the experiment. Layer 3 showed a similar trend until day 5, but between day 5 and day 10, the value of the layer decreased by 21%. The upper layers further away from the manure layer (1, 2) showed smaller values at day 5 and day 10 than the initial values. The last layer (7) showed increasing contents between the initial value and day 5, and decreased between day 5 and day 10. The average $NO_3^-$ concentrations of the whole soil column of the different treatments were of the same magnitude (Table 3), but there were some significant differences between the treatments. S60 had a significantly lower $NO_3^-$ concentration of ~22% (Table 3). The $NO_3^-$ concentration of I60 treatment was ~13% lower than the average of the other treatments. Treatments S40 and I60 also showed similarities with each other, but I40, I60 and also S40 and S60 differed from each other (Table 3).

#### 3.1.2. Spatial and Temporal Changes in $NH_4^+$ Concentration

In the 0 to 10 cm layer of the C40 treatment, $NH_4^+$ decreased by 29% from the initial content of 0.9 mg N $kg^{-1}$ throughout the experiment, while C60 exhibited a decrease of up to 33% until day 10 (Figure S2).

The S40 and S60 treatments showed a similar dynamic in $NH_4^+$ content during the experiment. S40 and S60 showed significantly increased $NH_4^+$ contents in the first manure-treated layer, and to a lesser extent, also in the second and third layers, until day 5. At day 10, the $NH_4^+$ value at S40 was 22% lower, while at S60 it was 29% lower in layer 1.

On day 5, the $NH_4^+$ content of the central, manure-treated layer 4 in I40 and the adjacent layers (3, 4) increased significantly compared with the initial content. The $NH_4^+$ content in layers 4 and 5 decreased by 35% and 32% between day 5 and day 10, respectively.

For I60, similar to I40, the $NH_4^+$ content of the manure-treated layer 4 and the neighbouring layers (3, 5) exhibited a strong increase over the first five days. Between day 5 and day 10, the $NH_4^+$ content of layer 3 decreased by 58%, and layers 4 and 5 decreased by 37% and 23%, respectively. Layers further away from the manure layer (1, 2, 6 and 7) in I40 and I60 showed decreasing values the further they were from layer 4. The average $NH_4^+$ concentrations of the surface treatments were 100 times higher, and the injected treatments were 60 times higher than the controls (Table 3). There was a significant effect from the method of manure application (surface or injected) on the $NH_4^+$ concentration. The mean $NH_4^+$ values of the S40 and S60 treatments, and also the I40 and I60 treatments showed similarities with each other (see the superscript letters in the Table 3 caption).

### *3.2. WEOC, Water Content, Gas Diffusivity and pH*

The WEOC content in the 0 to 10 cm layer of the C40 and C60 treatments decreased by 24% and 12% compared with the initial content of 8.66 mg N $ha^{-1}$ throughout the experiment.

In S40 there was a significant decrease in WEOC of 50% of the first, manure-treated layer between day 5 and day 10, while the deeper layers showed only small changes and differences from the initial value (Figure S3).

In S60, on day 5 and day 10, WEOC in the first layer containing the manure was higher than in S40. The decrease between day 5 and day 10 was 32%. The second layer WEOC was slightly higher than the values for layers 3 and 4 (Figure S3).

The WEOC of the manure-treated layer 4 in I40 decreased by more than 58% between day 5 and day 10.

In I60, the WEOC of the manure-treated layer 4 and the adjacent layer 3 above exhibited a strong increase in the first five days (Figure S3). Between day 5 and day 10, the WEOC of layer 3 decreased by 47%, and that of layer 4 decreased by 42%. Layer 5 experienced a 27% decrease between day 5 and day 10.

The average WEOC of the S60 treatment showed a significant difference compared to all of the other manure treatments (Table 3).

At 40% WFPS, the water content of the manure layers was distinct from the adjacent layers, showing that the water of the slurry did not move into the upper or lower layers. The gravimetric water content (GWC) was lowest in C40 (Figure S4). The GWC of C40 was 6% lower between day 5 and day 10. The GWC of C60 did not change over time. The slurry-treated layers in S40 had on average a 26% higher GWC, and S60 had a 17% higher GWC than the soil below. The manure-treated central layer 4 of I40 had, on average, a 39% higher GWC, and I60 had a 28% higher GWC than the other layers below or above.

The calculated gas diffusivity ($D_p/D_o$) corresponded (inverse) to the GWC because the treatments had the same bulk density (Figure S5).

The pH of the control soils was below 5 (Table 3). The average pH of the manure-treated soils was ~5–8% higher (Table 3) than the control. The pH of the manure-treated layers was 20–30% higher (Figure S6), and thus was significantly higher ($p < 0.001$) than the control. The effect of the manure treatments on the pH values of the nearby layers was small and insignificant, and negligible in the more distant layers.

### 3.3. $CO_2$ and $CH_4$ Fluxes

$CH_4$ fluxes were always below the level of detection.

The $CO_2$ flux dynamics of the control treatments moisture levels were comparable (Figure 1). All manure-treated soils had a similar emission pattern and magnitude, reaching a maximum after 2–3 days and then decreasing until day 4. The S40 and I40 treatments had higher and shorter $CO_2$ emission peaks than S60 and I60.

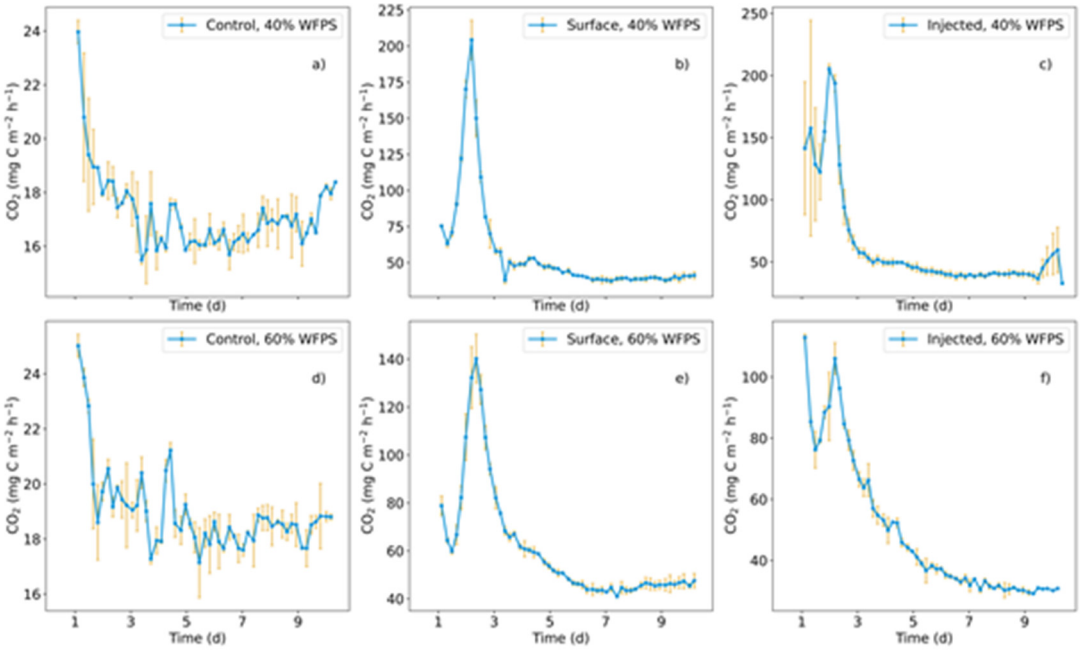


**Figure 1.** $CO_2$ fluxes during laboratory incubation of a sandy, arable soil from Fuhrberg, Germany. The water content (40% (**a**–**c**) and 60% (**d**–**f**) WPFS) was kept constant during the experiment. Three manure treatments were applied: control (no manure) (**a**,**d**), surface (manure on the surface) (**b**,**e**) and injected (manure in the middle layer of the soil core) (**c**,**f**). The yellow lines represented the standard deviation of the three parallel measurements. The first visualised measurement was taken within 18 h of the soil columns being packed.

The mean daily $CO_2$ emission of the manure-treated soil showed a significant difference from the controls ($p < 0.05$, Table 4). Of the manure-treated soils, only S60 and I60 ($p = 0.011$) and I40 and I60 ($p = 0.0033$) differed from each other (Table 4).

**Table 4.** Average daily fluxes of $CO_2$, total $N_2O$ ($N_2O_T$), of $N_2$ ($fp\_N_2$) and $N_2O$ ($fp\_N_2O$) originating from the $^{15}N$-labelled $NO_3^-$ pool and $N_2O$ from other sources ($N_2O_{os}$). Daily average values of $fp\_N_2 + fp\_N_2O$ and $fp\_N_2 + N_2O_T$ (in mg N $m^{-2}$ $day^{-1}$; $CO_2$: g C $m^{-2}$ $day^{-1}$) are also given over a 10-day laboratory incubation of sandy soil with two WFPS (40% and 60%) levels. Daily averages of a 10-day experiment are shown, and standard deviation of three replicate cores without (C40 and C60) manure, and with surface-applied (S40 and S60) and injected manure (I40 and I60). Superscript letters indicate significant differences within sites and between treatments ($p < 0.05$; Tukey HSD, n = 3).

| | C40 | C60 | S40 | S60 | I40 | I60 |
|---|---|---|---|---|---|---|
| $fp\_N_2$ | 0.09 | $0.51 \pm 0.12^{a}$ | $0.45 \pm 0.28^{a}$ | $7.59 \pm 7.70^{b}$ | $0.692 \pm 0.38^{a}$ | $33.0 \pm 31.5^{c}$ |
| $fp\_N_2O$ | 0.06 | $2.22 \pm 1.58^{a}$ | $0.22 \pm 0.13^{b}$ | $13.6 \pm 11.4^{c}$ | $0.340 \pm 0.20^{b}$ | $36.1 \pm 39.1^{d}$ |
| $N_2O_T$ | $0.08 \pm 0.004^{a}$ | $4.77 \pm 0.56^{d}$ | $0.39 \pm 0.06^{b}$ | $20.9 \pm 2.95^{e}$ | $0.61 \pm 0.05^{c}$ | $49.8 \pm 0.35^{f}$ |
| $N_2O_{os}$ | 0.08 | $1.06 \pm 0.31^{b}$ | $0.19 \pm 0.08^{ab}$ | $1.01 \pm 1.07^{ab}$ | $0.36 \pm 0.15^{a}$ | $2.21 \pm 3.31^{b}$ |
| $fp\_N_2 + fp\_N_2O$ | 0.15 | $2.73 \pm 1.70^{ab}$ | $0.68 \pm 0.41^{a}$ | $21.2 \pm 19.1^{bc}$ | $1.03 \pm 0.57^{a}$ | $69.1 \pm 70.6^{c}$ |
| $fp\_N_2 + N_2O_T$ | $0.80 \pm 0.02^{a}$ | $3.72 \pm 1.27^{ab}$ | $1.56 \pm 0.54^{a}$ | $22.7 \pm 17.9^{bc}$ | $1.91 \pm 0.47^{a}$ | $69.8 \pm 54.6^{c}$ |
| $N_2Oi$ | $0.49 \pm 0.22$ | $0.79 \pm 0.09$ | $0.34 \pm 0.07$ | $0.65 \pm 0.17$ | $0.34 \pm 0.14$ | $0.52 \pm 0.03$ |
| $CO_2$ | $0.41 \pm 0.01^{a}$ | $0.46 \pm 0.01^{a}$ | $1.36 \pm 0.05^{bc}$ | $1.45 \pm 0.05^{b}$ | $1.51 \pm 0.19^{b}$ | $1.18 \pm 0.03^{c}$ |
| $fp\_N_2$ | 0.09 | $0.51 \pm 0.12^{a}$ | $0.45 \pm 0.28^{a}$ | $7.59 \pm 7.70^{b}$ | $0.692 \pm 0.38^{a}$ | $33.0 \pm 31.5^{c}$ |

### *3.4. $N_2O$, $N_2$ Fluxes and Product Ratio of Denitrification*

$N_2O_T$ was low ($0.36 \pm 0.27$ mg N $m^{-2}$ $day^{-1}$) in the dry treatments and was 13 times higher ($p < 0.0001$) in the wet control (C60) (Table 4). The wet manure treatments ($25.2 \pm 22.8$ mg N $m^{-2}$ $day^{-1}$) were 70 times higher than the dry treatments, with the highest values being found in I60. A similar pattern, but with even greater differences, was found in $fp\_N_2O$, $fp\_N_2$ and $fp\_N_2 + fp\_N_2O$, where the wet treatments were 83, 33 and 50 times higher, respectively, than the dry treatment. For $N_2O_{os}$, the average difference between the dry and wet treatments was negligible.

The product ratio of denitrification ($N_2Oi = fp\_N_2O/(fp\_N_2 + fp\_N_2O)$) was higher at high moisture (0.52 to 0.79, 60% WFPS) compared with the drier treatments (0.34 to 0.49, 40% WFPS), and was lower in the slurry treatments than in the control.

The time course with a sub-daily resolution of C40 showed a constantly low value of $N_2O_T$ (Figure 2), while S40 and I40 showed a clearly increasing trend. I40 had a small but broad peak between days 4 and 7. C60 had the maximum emission on the second day and thereafter, the flux decreased almost constantly. The S60 treatment showed a rapid increase in $N_2O_T$ in the first four days. I60 had the highest $N_2O_T$, which was measured between days 4 and 5.

The temporal pattern of $fp\_N_2O$ with bi-weekly resolution showed a very small emission from C40. The $fp\_N_2O$ had an increasing trend in manure-treated S40 and I40. In the wet treatments, the $fp\_N_2O$ was almost always equal to the $N_2O_T$. Initially, C60, S60 and I60 had low $fp\_N_2O$ values, but these rapidly increased during the first five days of incubation. The $fp\_N_2O$ was the dominant emitted N throughout the experiment for C60 and S60. With I60, $fp\_N_2O$ was the dominant emitted N form until day 7.

$N_2O_{os}$ and $fp\_N_2O$ had a similar magnitude in the dry treatments. $N_2O_{os}$ also showed a slowly increasing trend between day 5 and day 10 in S40 and I40. In the wet treatments, $N_2O_{os}$ was very small compared with the $fp\_N_2O$.

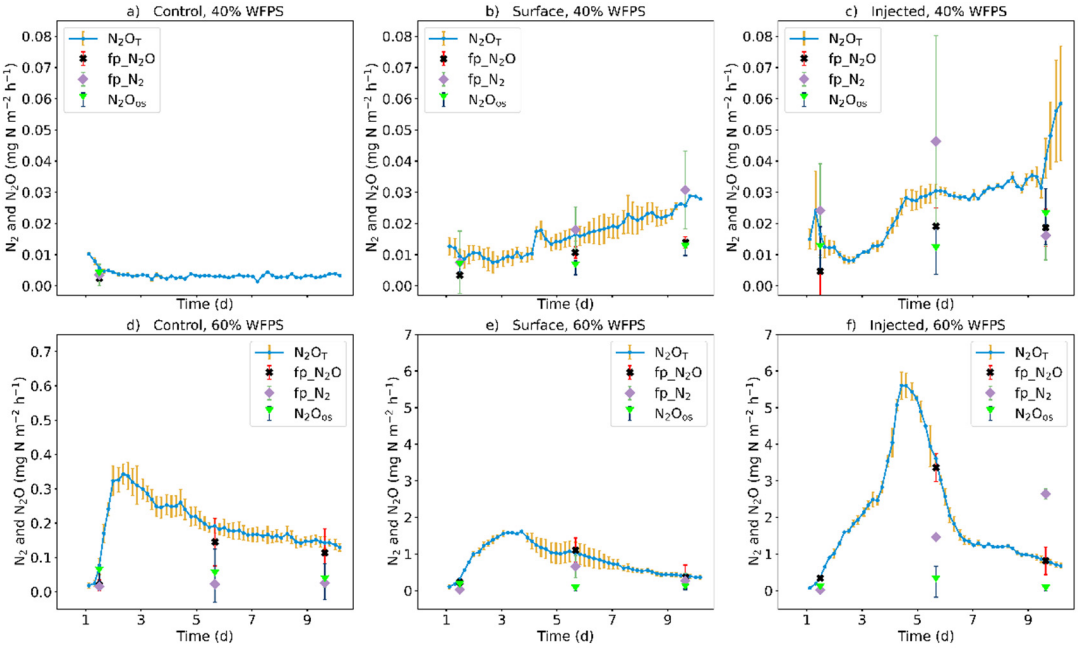


**Figure 2.** Measured total $N_2O$ flux ($N_2O_T$; blue line, continuous GC measurement), fp_$N_2$ (purple dots; $^{15}$N-sampling), fp_$N_2O$ (black dots; $^{15}$N-sampling) and $N_2O_{os}$ (green dots; $N_2O_T$-fp_$N_2O$) during a laboratory incubation of a sandy, arable soil from Fuhrberg, Germany. The water content (40% (**a**–**c**) and 60% (**d**–**f**) WPFS) was kept constant during the experiment. Three manure treatments were applied: control (no manure) (**a**,**c**), surface-applied manure (manure on the surface) (**b**,**d**) and injected manure (manure in the middle layer of the soil) (**c**,**f**). The yellow lines represented the standard deviation of the three parallel measurements. The first visualised measurement was taken within 18 h of the soil columns being packed.

The fp_$N_2$ flux was below detection in the C40 treatment, except for the low value detected on day 1. The fp_$N_2$ showed an increasing trend in S40 throughout the experiment. In I40, the temporal pattern of fp_$N_2$ was at its maximum on day 5 (Figure 2). In C60, the fp_$N_2$ was constantly low. In S60, the fp_$N_2$ was at its maximum on day 5. The flux had a similar pattern to fp_$N_2O$, but tended to be lower. The fp_$N_2$ of I60 showed an increasing trend throughout the experiment, and at the end, the fp_$N_2$ flux was 224% higher than the fp_$N_2O$ flux.

The time course of $N_2Oi$ (Figure S7) showed that in I40, this ratio was lower at the start, but that it increased during the experiment, while S40 exhibited the opposite trend. The $N_2Oi$ of S60 and I60 were almost identical at day 1 and day 5, while in S60 the decreasing trend stopped between day 5 and day 10; in I60, $N_2Oi$ decreased further almost linearly until day 10. The trend of C60 was opposite to that of S60.

### *3.5. $^{15}$N Enrichment of $NO_3^-$ and Gross Nitrification Rate*

The $^{15}$N enrichment of extracted (total) $NO_3^-$-N ($^{15}aNO_3$) exhibited decreasing trends in all treatments (Figure S8), indicating dilution by $NO_3^-$ that was produced by nitrification. $^{15}$N enrichment of the $NO_3^-$ pool undergoing $N_2O$ production by denitrification ($apN_2O$) was always higher than $^{15}aNO_3$, especially in S60 and I60, showing that the N pools undergoing denitrification were less diluted with unlabelled $NO_3^-$ compared to the bulk soil (Figure S9). $^{15}$N enrichment of the $NO_3^-$ pool undergoing $N_2$ production by denitrification ($apN_2$) was only detectable when fp_$N_2$ was high, and it was mostly close to $apN_2O$ (data not shown).

$^{15}aNO_3$ was used to calculate the gross nitrification rates (GNR). The controls had the lowest GNR, but a higher GNR in the wetter treatment (Figure S10; C40: 0.323 mg N $kg^{-1}$ $day^{-1}$;

C60: 0.626 mg N $kg^{-1}$ $day^{-1}$). All layers of manure treatments showed higher levels of GNR than the controls.

The first manure layer of the S40 treatment had the second-highest GNR (4.30 mg N $kg^{-1}$ $day^{-1}$), with GNR decreasing constantly from the first to the last layer. The GNR of the first three layers of the S60 treatment were similar at around 2.5 mg N $kg^{-1}$, and higher than the bottom layer.

The I40 treatment generally had the highest GNR in the fourth, middle, manure-treated layer (4.43 mg N $kg^{-1}$ $day^{-1}$). The upper and lower layers decreased almost in parallel with increasing distance from the middle layer. The top layer of the I60 treatment had the highest GNR value among the 60% WFPS treatments (3.44 mg N $kg^{-1}$ $day^{-1}$). The second and fourth layers were around 20% lower, and the other layers were 50–70% lower than the top layer.

## 4. Discussion

### *4.1. Manure Effect on Depth Distribution of WEOC, pH and Water Content*

The WEOC content was elevated in the manure-treated soil layers, providing an ideal carbon supply for denitrification [35]. The turnover of labile carbon is important for denitrification, due to the enhancement of anoxic microsites by $O_2$ consumption by respiration, and as an electron donor for denitrifying microbes [15,16]. The increased respiration as expressed by the high $CO_2$ fluxes could have been responsible for the decreasing trends in WEOC concentration between day 5 and day 10. The increased WEOC content of the manure-amended layer only increased the WEOC concentration of the nearby layers to a small extent. This can be explained by the relatively high water retention of the cattle slurry and therefore by a low-to-moderate rate of solute (WEOC, $N_{min}$) transport to the surrounding soil layers [25,28].

The manure amendment in the dry treatments increased the water content of the soil (Figure S4) in the treated layer. Water movement between the manure-treated and the nearby soil layers was evident in the wet treatments, but not in the dry treatments. This can be attributed to the low unsaturated hydraulic conductivity of sandy soils under dry conditions [59] and the high water-retention capacity of the cattle slurry [32] that was apparently not sufficient to retain all of the water in the wet treatment. The differences in water content between the layers of the wet treatments can be traced back directly to seepage due to the extra water added to achieve 60% WFPS, and the water content of the added manure. The joint effect of these processes explains the observed gradients in the water content (Figure S4).

The higher pH of the manure-treated layers can be traced back to the higher pH of the manure.

In line with hypothesis (i), the pH and soil water, labile C and $NH_4^+$ content of the surrounding soil increased due to the manure treatment.

### *4.2. Manure Effect on the Depth Distribution of Mineral N and Nitrification*

The differences in $NH_4^+$-N and $NO_3^-$-N between treatments and sampling dates resulted from the input (via manure), N transformations (mineralisation, nitrification, denitrification and immobilisation) and gaseous or leaching losses [60].

The N input with manure was reflected in the increased concentration of $NH_4^+$ after five days in, and adjacent to the manure layers in all of the manure-treated soils. Elevated values in the adjacent layers can be attributed to the migration of manure $NH_4^+$ by diffusion and/or mass flow with the liquid phase of the manure.

The differences in the $NO_3^-$-N (and $NH_4^+$-N) concentrations of the 40% WFPS treatments at days 5 and 10 between untreated and manure-treated soils (Figures S1 and S2) were due to the nitrification of $NH_4^+$ in the manure, whether it was $NH_4^+$ that was initially present in the applied manure, or additional $NH_4^+$ produced from organic N. This could be accounted for by the gross nitrification rates (GNR) calculated from the dilution of the added $^{15}N$–labelled $NO_3^-$ by non-labelled $NO_3^-$ from nitrification (Figure S10). Nitrifica-

tion rates decline at a high soil-water content because the presence of $O_2$ is essential for this process, and the low water content and well-aerated soil provide more suitable conditions for nitrification [61]. The optimum WFPS for nitrification is around 40% for coarse, sandy soil [62]. The two upper layers of the S60 treatment had close contact with the atmosphere and thereby a constant $O_2$ supply, which in combination with the high $NH_4^+$ concentration resulted in the highest GNR overall.

GNR was higher with a lower soil moisture, and it was highest in the manure-treated layer. The GNR showed an almost linear decrease with distance from the manure layer in dry soil, coinciding with $NH_4^+$-N availability by day 5 (Figure S2), clearly showing that GNR depended on the $NH_4^+$ content. The increased substrate availability (see Section 3.1.2) in the manure-treated layers and the available $O_2$ as a result of the lower 40% WFPS created the ideal conditions for nitrification processes [61]. The patterns of the GNR closely followed the decreasing $NH_4^+$ and increasing $NO_3^-$ concentrations in the layers in the 40% WFPS and the 60% WFPS surface treatments. Although the diffusion coefficient of the manure-amended layer was within a range that could lead to $O_2$ limitation [25,63], the adjacent soil layers had higher $D_p/D_o$ values. The soil water did not block $O_2$ diffusion to the manure-treated layer, and the nitrification process was not blocked completely.

Nitrate-N depletion until day 5 in the upper layers of the treatment with surface-applied manure could be due to the combined effects of leaching (induced by manure liquid and also by watering of the wet treatment) and denitrification (induced by respiration and C supply from the manure) [64]. This effect was more pronounced in the wet treatment (S60) because more liquid was added, and the denitrification rates were much higher (Table 4). The loss of mineral N in I60 and S60 during the incubation of 6.3 mg N $kg^{-1}$ and 17.8 mg N $kg^{-1}$ was larger than the gaseous fluxes of 3.32 mg N $kg^{-1}$ and 1.39 mg N $kg^{-1}$. This suggests that the drastically decreased initial $NO_3^-$ value until day 5 and the increased value at day 10 could imply other soil processes as well. The immobilisation of a significant part of added mineral $NO_3^-$ and re-mineralisation—with the presence of a high concentration of organic matter—could be significant in the soil–manure boundary layers [54,65]. The high water content and the high labile carbon availability in the soil–manure boundary layer could shift the dominant $NO_3^-$ consumption from denitrification to dissimilatory nitrate reduction to ammonium (DNRA) [66,67].

The manure-treated layer of S40 and I40 showed a high GNR between days 5 and 10, and this resulted in an increased $NO_3^-$-N concentration.

In the wet manure treatments (S60 and I60), the highest $NO_3^-$-N values were measured in the lower layers, apparently due to leaching after wetting of the soil at the start of the experiment, since drainage was indicated by the gradient of water content [68]. This hypothesis (ii) was confirmed, since the $NO_3^-$ concentration increased due to gross N nitrification in the manure-treated layers.

### *4.3. Manure Effect on $CO_2$ Fluxes*

The $CO_2$ fluxes of all the manure treatments were much higher than those of the controls, due to enhanced respiration induced by the labile organic C of the manure [69]. On Day 1, the $CO_2$ fluxes showed a declining trend. There was a maximum of three hours between the close of the soil columns and the first measurement event. It was assumed that there are several reasons for this trend. As well as the added extra water and $NO_3^-$, soluble C could infiltrate the soil after a few hours of soil packing, which could cause an initial peak in respiration. Another reason could be the $CO_2$ that was derived from $CO_3^{2-}$, when the high pH of the added manure is buffered by the soil [70].

While the magnitude and time course of the fluxes were similar in the manure treatments, the well-aerated 40% WFPS treatments exhibited higher and thinner $CO_2$ peaks than the 60% WFPS treatments (Figure 1). These peaks between days 2 and 3 might reflect the microbial growth phase. However, the reason for the relatively fast decline of the $CO_2$ fluxes could be substrate and/or $O_2$ limitation. Decomposition rates in the 60% WFPS

treatments were lower, as expressed by the lower $CO_2$ fluxes due to reduced soil aeration compared with the 40% WFPS treatments (Table 4, Figure S5) [23,71].

### *4.4. Manure Effect on $N_2$ and $N_2O$ Processes and Fluxes*

To the authors' knowledge, this is the first time that the effect of surface and injected manure application on $N_2$ + $N_2O$ production and $N_2Oi$ has been investigated.

In line with the 60% WFPS treatments results, the enhancement of $N_2O_T$ by manure injection has been reported by Duncan et al. (2017) [72]. They measured an 84% to 152% higher $N_2O_T$ flux with injected manure application than the surface-applied manure. In the I60 treatment, a 138% higher $N_2O_T$ flux was observed with a simulated injection, compared with the surface application.

All flux types consisting of or including gaseous denitrification products (i.e., $N_2O_T$, fp_$N_2$, fp_$N_2O$ and fp_$N_2$ + fp_$N_2O$) showed significant differences between the different manure and water applications, where fluxes of the wet treatments were several times higher than the 40% WFPS treatments (Table 4). This is in line with the well-known impact of soil moisture and labile carbon on denitrification [11–13,18]. While increasing moisture in the absence of manure yielded approximately four times more fp_$N_2$ + $N_2O$ fluxes, manure treatments exhibited up to 40 times higher denitrification rates (given by fp_$N_2$ + fp_$N_2O$) than the dry control. The manure effect is known to be a combined moisture and labile carbon effect, since the slurry placement likely caused locally increased respiration and higher water contents around the manure-amended layers, which induce local anaerobic hotspots [32] where denitrification occurs. The water transport from the manure to the surrounding soil with a high concentration of soluble labile organic C and mineral N resulted in a higher respiration rate, nitrification and locally decreased $O_2$ concentration. This water transport also increased the concentration of the electron donors (WEOC) and electron acceptors ($NO_3^-$) [29,33,73].

In the 40% WFPS manure treatments, the relatively low water content resulted in high gas diffusivity ($D_p/D_o > 0.045$, Figure S5) and thus good conditions for gas exchange [74,75]. However, the enhancement of denitrification (increased fp_$N_2$ and fp_$N_2O$) by the manure was evident towards the end of the experiment (Figure 2). There was also a difference in the fp_$N_2$ + fp_$N_2O$ values between the surface and injected treatments. I40 had 25% higher fp_$N_2$ + fp_$N_2O$ than S40. This was probably due to the inhibited aeration of I40 compared with S40, due to the greater distance between the manure layer and the soil surface, which may even have been enhanced by the 14% lower diffusion coefficient.

The denitrification process was the dominant soil process of the total $N_2O$ flux in the 60% WFPS treatments [76,77], but the effect of the manure and the application method (surface or injected) also had a remarkable effect.

The locally limited $O_2$ diffusion could be also the main reason for the differences between the surface and injected treatments at 60% WFPS. The lowering of the diffusion coefficient by the increased water content in the manure-amended layers in S60 and I60 was in the range that was reported for conditions where diffusion processes are almost or fully blocked [74,75]. While gas diffusion of the adjacent layers was not completely blocked, it was smaller than the diffusion of the 40% WFPS treatments. This resulted in slow $O_2$ transport to the deeper layers in 60% WFPS treatments, and the locally developed anoxic hotspots around the manure layers resulted in high denitrification rates.

The extent of $N_2O$ reduction to $N_2$, as shown by the $N_2O/(N_2 + N_2O)$ product ratio of denitrification ($N_2Oi$), was affected by moisture and the manure treatment. The dry treatments exhibited the highest $N_2Oi$ with values > 0.5, showing that the dominant product was $N_2O$. This could be due to the low pH of the soil, which can inhibit $N_2O$ reduction to $N_2$ [78], and/or because $N_2O$ reduction was not enhanced by the known effects of high moisture [24]. The manure-treated soils resulted in elevated fp_$N_2$ flux relative to fp_$N_2O$, and thus lower $N_2Oi$. The differences between the control and manure-treated $N_2Oi$ values can be explained by the interaction of multiple manure effects, including increased water and solute (WEOC, mineral N) content near the manure, and anoxia

resulting from increased $O_2$ consumption by the respiration of labile C from manure, the latter also supplying reductants for denitrifiers [79]. While all of these factors enhance $N_2$ and $N_2O$ production by denitrification and increased pH, increased moisture and the abundance of labile carbon in the soil surrounding the manure are factors that can enhance $N_2O$ reduction and thus lower $N_2Oi$, which might explain the lower $N_2Oi$ values of the manure treatments.

Another factor could be the delayed formation of the $N_2O$ reductase [80–83], which was evident in the wet injection treatment (I60) (Figure S7). Moreover, this treatment was lower (−20%) in $N_2Oi$ than the wet surface manure treatment (S60), possibly due to the longer residence time of $N_2O$ in the soil when the manure hotspot was located 5 cm below the soil surface.

It should be noted that the extent to which the lower $N_2Oi$ levels in the injected treatment was due to enhanced moisture, labile carbon or elevated pH, and how this was counteracted by a higher $NO_3^-$ concentration, is unclear from the data. Further studies are necessary to elucidate the full regulation of $N_2Oi$ after manure application.

The total $N_2O$ flux also included variable contributions from processes other than denitrification ($N_2O_{os}$) [84]. The approach used here only distinguished $N_2O$ that was evolved from the $NO_3^-$-labelled pool (denitrification) from other sources, which could have originated from autotrophic or heterotrophic nitrification or nitrifier denitrification [24,85]. $N_2O$ from autotrophic nitrification is expected to be relevant, since large amounts of $NH_4^+$ were transformed into $NO_3^-$, whereas in I40 and I60, only a minor part, and in S40 and S60, a significant part of the initially added 85.7 kg $NH_4^+$-N $ha^{-1}$ was recovered as $NH_4^+$, largely due to nitrification, as shown by the high GNR values of the manure treatments (Figure S10). The $N_2O$ yield of autotrophic nitrification varies from approximately $0.5 \times 10^{-3}$ to $1 \times 10^{-3}$ mg $N_2O$-N per mg of nitrified $NH_4^+$-N [86], which would lead to an $N_2O$ flux of up to 0.4 to 0.8 mg N $m^{-2}$ $day^{-1}$ (80 kg nitrified $NH_4^+$-N $ha^{-1}$ $\times$ ($0.5 \times 10^{-3}$ to $1 \times 10^{-3}$)). This is lower than the $N_2O_{OS}$ of the 60% WFPS treatments (Table 4). Moreover, $N_2O_{OS}$ was not clearly enhanced in the manure treatments, showing that processes other than autotrophic nitrification during the oxidation of manure $NH_4^+$, such as nitrifier denitrification or heterotrophic nitrification [85], might have been relevant. However, $N_2O_{OS}$ was low compared with $N_2O$ from the denitrification of the labelled $NO_3^-$ (fp_$N_2O$), showing that the inability to apportion $N_2O_{OS}$ to its source processes was not a major limitation of this study.

### *4.5. Manure Effect on the Depth Distribution of WEOC, pH and Water Content*

The data demonstrated how the dynamics of moisture, labile organic C, $NO_3^-$-N, $NH_4^+$-N, the formation of $NO_3^-$-N by nitrification and pH following manure surface or injection application interact and result in $N_2O$ cycling by various pathways. The manure–soil boundary layer can be defined as a hotspot for C and N cycling, since the manure application generated an increase in water content, mineral N and labile C availability in the 1–4 mm of soil adjacent to the manure-saturated soil where microbial activity and $O_2$ demand were also increased [15,87,88]. As hypothesised, the manure increased the pH and the water content with labile C and $NH_4^+$ together in the surrounding soil of the manure layer (hypothesis (i)). This resulted in increased denitrification within the first five days, but the soil-derived $NO_3^-$ became limited. The decreased $NO_3^-$ until day 5 and the increased $NO_3^-$ concentration between days 5 and 10 in S60 (Figure S1), in line with the GNR (Figure S10) through the nitrification processes showed similarities with the results of the Petersen et al. (1996) [29] (hypothesis (ii)). The present study's data confirmed the well-known dynamics of nitrification, coupled with denitrification in manure hotspots [89], since both enhanced GNR in manure layers and manure-induced denitrification were found. The $O_2$ demand was apparently higher than the supply through diffusion, and the denitrification process again became dominant in the anaerobic microsites of the manure-amended layers. Due to the nitrification of $NH_4^+$ from the manure, the $NO_3^-$ concentration increased and was no longer the limiting factor for denitrification. In a similar incubation

study with manure hotspots [29], after seven days, the limiting factor for denitrification was the available labile C source. Although the WEOC concentration decreased during the 10-day experiment (Figure S3), the WEOC value of the manure-treated layer was still high. Hence, WEOC did not suggest a limitation, and it would seem that denitrification was not limited by the substrates. Nevertheless, local WEOC could be limited in the microsites of the soil–manure boundary layer (hypothesis (iii)). $N_2O$ reduction to $N_2$, and thus to $N_2Oi$, is due to the interaction of multiple factors, i.e., all of the main factors controlling denitrification, but also pH, residual $O_2$, the temporal dynamics of $N_2O$ reductase formation and the physical factors of $N_2O$ exchange [24,38]. Although a reduction in $N_2Oi$ towards the end of the incubation was observed in the wet manure treatments (confirming hypothesis iv), it is not clear which combination of the aforementioned factors was relevant, because there was incomplete spatial information about the control factors, and the enzyme dynamics were not examined at all.

The fact that hypothesis (v) could not be fully or clearly verified, since there was no trend for lower $N_2Oi$ in the dry manure injection vs. the dry surface application treatments, is probably due to this complexity in $N_2Oi$ control. Inhibiting $N_2O$ reduction (Figure S8) by the delayed formation of $N_2O$ reductase [81,90] might have been more relevant for the injection treatment in view of the higher denitrification rate.

A model to describe manure-induced hotspot dynamics to simulate $N_2$ and $N_2O$ fluxes was proposed by Sommer et al. (2004) [40] and calibrated using incubations of manure-treated soils similar to the present setup, but without using $^{15}N$ tracing approaches [32,87]. This so-called "static model" calculates the following N transformations: $NH_3$ loss at the time of the manure application on the soil, N mineralisation in the degradable volatile solids, nitrification in the manure slurry clump and soil, and denitrification in the manure slurry clump. The present data provide the basis for extended evaluation and further development of such hotspot models, because in addition to the analysis of $CO_2$ and $N_2O$ fluxes, water content and N and C substrates, it includes information on gross nitrification and on $N_2O$ and $N_2$ fluxes from denitrification. The combined data from the repeated soil sampling and continuous gas fluxes can thus be used to describe the denitrification and respiration processes of the manure-soil hotspot. The data gave clear indications in this 10-day period about the manure-induced denitrification dynamics in sandy soil. However, only one soil type was tested. Moreover, with bi-weekly gas sampling for isotope analysis and soil sampling on only two dates, the temporal resolution was insufficient to monitor in detail the rapid manure-induced changes in the process dynamics (e.g., immobilisation, nitrification and denitrification, etc.). Finally, this setup could not differentiate between all of the $N_2O$ processes and did not yield spatial information on respiration, $O_2$ or pore structure. Therefore, for improved understanding and the prediction of the effects of the control factors on $N_2$ and $N_2O$ fluxes, longer and more frequent experiments are needed that feature more soil types, including additional techniques for distinguishing gross N transformations and their gaseous N fluxes [91], and tools to study the interaction of respiration, pores structure and spatial $O_2$ dynamics [92,93].

## 5. Conclusions

The objective of this study was to investigate the effect of different manure application techniques on $N_2$ and $N_2O$ fluxes and their control factors, and thus, to produce reliable data for evaluating a manure-soil hotspot model. The results of a mesocosm laboratory incubation were presented that explored the response of these fluxes to the combination of two water contents and two manure application methods. The results confirmed an expected increase in the content of water, labile organic carbon and mineral N, as well as nitrification in and next to the manure-treated soil layers. Moreover, these factors were found to increase the $N_2$ and $N_2O$ fluxes from denitrification, with the highest fluxes occurring in the wet manure injection treatment. A moderate enhancement of $N_2O$ reduction to $N_2$, and thus the lowering of the $N_2O/(N_2 + N_2O)$ product ratio of denitrification (with $28.3 \pm 7.24\%$ lower $N_2Oi$ on average) resulted from the wetting and

manure application, but this small effect could not balance the strong increase in gross $N_2O$ production. However, a lower soil-water content could mitigate the absolute value of $N_2O$ flux of the manure-amended soil. Since the spatial distribution of moisture, mineral N, WEOC, pH and continuous $CO_2$ fluxes as a proxy for respiration were assessed, it was possible to explain most of the observed $N_2$ and $N_2O$ flux patterns from the interaction of these control factors of denitrification and nitrification. It is assumed that the refined parameter determination, including pore structure, $O_2$ distribution and the higher temporal resolution of $N_2$ fluxes can lead to an even better explanation of flux patterns in future studies. It is concluded that the current dataset is suitable as a first step for improving biogeochemical models and their ability to predict manure application effects, but more refined experiments with different types of soils are needed.

**Supplementary Materials:** The following supporting information can be downloaded at: https://www.mdpi.com/article/10.3390/agriculture12050692/s1, Figure S1: Nitrate concentration differences in soil layers between days 1, 5 and 10 of sampling of the control (one layer), surface (four layers) and injected (seven layers) manure treatments for two water contents (40% and 60% WFPS) and the standard deviation of the three parallel samples. The laboratory incubation was conducted with re-packed, sandy, arable soil from Fuhrberg, Germany. Figure S2: Differences in the ammonium concentration in soil layers between day 5 and day 10 of sampling of the control (one layer), surface (four layers) and injected (seven layers) manure treatments for two water contents (40% and 60% WFPS) and the standard deviation of the three parallel samples. The laboratory incubation was conducted with re-packed, sandy, arable soil from Fuhrberg, Germany. Figure S3: Dissolved organic carbon concentration differences in soil layers between day 5 and day 10 of sampling for the control (one layer), surface (four layers) and injected (seven layers) manure treatments for two water contents (40% and 60% WFPS) and the standard deviation of the three parallel samples. The laboratory incubation was conducted with re-packed, sandy, arable soil from Fuhrberg, Germany. Figure S4: Gravimetric water content of soil layers between day 5 and day 10 sampling of the control (one layer), surface (four layers) and injected (seven layers) manure treatments for two water contents (40% and 60% WFPS), and the standard deviation of the three parallel samples. The laboratory incubation was conducted with re-packed, sandy, arable soil from Fuhrberg, Germany. Figure S5: The calculated gas diffusivity based on the measured water content of soil layers between day 5 and day 10 of the control (one layer), surface (four layers) and injected (seven layers) manure treatments for two water contents (40% and 60% WFPS). The laboratory incubation was conducted with re-packed, sandy, arable soil from Fuhrberg, Germany. Figure S6: The pH of soil layers between day 5 and day 10 of the control (one layer), surface (four layers) and injected (seven layers) manure treatments for two water contents (40% and 60% WFPS). The laboratory incubation was conducted with re-packed, sandy, arable soil from Fuhrberg, Germany. Figure S7: Time course of $N_2Oi$ ($fp\_N_2O/(fp\_N_2 + fp\_N_2O)$ at days 1, 5 and 10 of the control, surface and injected (C, S, I) manure treatments for two water contents (40% and 60% WFPS). The laboratory incubation was conducted with re-packed, sandy, arable soil from Fuhrberg, Germany. Figure S8: The $^{15}N\text{-}NO_3^-$ atom% of soil layers between days 1, 5 and 10 of the control (one layer), surface (four layers) and injected (seven layers) manure treatments for two water contents (40% and 60% WFPS). The laboratory incubation was conducted with re-packed, sandy, arable soil from Fuhrberg, Germany. Figure S9: The $apN_2O$ values between days 1, 5 and 10 of the control, surface and injected manure treatments for two water contents (40% and 60% WFPS). The laboratory incubation was conducted with re-packed, sandy, arable soil from Fuhrberg, Germany. Figure S10: The gross nitrification rate of soil layers between day 5 and day 10 of the control (one layer), surface (four layers) and injected (seven layers) manure treatments for two water contents (40% and 60% WFPS). The laboratory incubation was conducted with re-packed, sandy, arable soil from Fuhrberg, Germany. Table S1: Physical and chemical data of four-week-old matured artificial manure mixture. See [45,48,49,94–96].

**Author Contributions:** B.G., S.O.P. and R.W. designed the experiment. B.G., S.B. and B.K. conducted the experiment. B.G. prepared the manuscript with contributions from all co-authors. All authors have read and agreed to the published version of the manuscript.

**Funding:** This study was funded by the Deutsche Forschungsgemeinschaft (DFG)—Project number: 420651168: Modelling the Impact of Liquid Organic Fertilization and associated Application Tech-

niques on $N_2O$ and $N_2$ Emissions from Agricultural Soils (MOFANE). https://gepris.dfg.de/gepris/projekt/420651168?language=en (accessed on 10 May 2022).

**Institutional Review Board Statement:** Not applicable.

**Informed Consent Statement:** Not applicable.

**Data Availability Statement:** The mesocosm experiment data are available from the authors on request.

**Acknowledgments:** This study was funded by the Deutsche Forschungsgemeinschaft (DFG)—Project number: 420651168: Modelling the Impact of Liquid Organic Fertilization and associated Application Techniques on $N_2O$ and $N_2$ Emissions from Agricultural Soils (MOFANE). We thank the laboratory teams of the Institute of Soil Science, Centre for Stable Isotope Research and Analysis of Göttingen University and Thünen Institute of Climate-Smart Agriculture, Braunschweig, for support in analysis and experiments, respectively. Specifically, we thank Martina Heuer, Ute Rieß, Jennifer Giere and Jens Dyckmans for isotopic analyses, Ute Tambor and Sabine Watsack for further analysis and sampling, and Stefan Burkart for supporting automated incubations.

**Conflicts of Interest:** The authors declare no conflict of interest.

## References

1. Erisman, J.W.; Galloway, J.; Seitzinger, S.; Bleeker, A.; Butterbach-Bahl, K. Reactive Nitrogen in the Environment and Its Effect on Climate Change. *Curr. Opin. Environ. Sustain.* **2011**, *3*, 281–290. [CrossRef]
2. Bernal, M.; Bescós, B.; Burgos, L.; Bustamante, M.A.; Clemente, R.; Fabbri, C.; Flotats, X.; García-González, M.C.; Herrero, E.; Mattachini, G.; et al. *Evaluation of Manure Management Systems in Europe*. 2015. Available online: https://upcommons.upc.edu/handle/2117/88745 (accessed on 4 May 2022).
3. Buckwell, A.; Nadeu, E. *Nutrient Recovery and Reuse (NRR) in European Agriculture. A Review of the Issues, Opportunities, and Actions*; RISE Foundation: Brussels, Belgium, 2016.
4. Köninger, J.; Lugato, E.; Panagos, P.; Kochupillai, M.; Orgiazzi, A.; Briones, M.J.I. Manure Management and Soil Biodiversity: Towards More Sustainable Food Systems in the EU. *Agric. Syst.* **2021**, *194*, 103251. [CrossRef]
5. Galloway, J.N.; Dentener, F.J.; Capone, D.G.; Boyer, E.W.; Howarth, R.W.; Seitzinger, S.P.; Asner, G.P.; Cleveland, C.C.; Green, P.A.; Holland, E.A.; et al. Nitrogen Cycles: Past, Present, and Future. *Biogeochemistry* **2004**, *70*, 153–226. [CrossRef]
6. Culman, S.; Fulford, A.; Camberato, J.; Steinke, K.; Lindsey, L.; LaBarge, G.; Watters, H.; Lentz, E.; Haden, R.; Richer, E.; et al. Tri-State Fertilizer Recommendations. 1995. Available online: https://agcrops.osu.edu/FertilityResources/tri-state_info (accessed on 4 May 2022).
7. Ravishankara, A.R.; Daniel, J.S.; Portmann, R.W. Nitrous Oxide ($N_2O$): The Dominant Ozone-Depleting Substance Emitted in the 21st Century. *Science* **2009**, *326*, 123–125. [CrossRef] [PubMed]
8. Flessa, H. *Minderung von Stickstoff—Emissionen aus der Landwirtschaft—Empfehlungen für die Praxis und Aktuelle Fragen an die Wissenschaft*; Senat der Bundesforschungsinstitute des Bundesministeriums für Ernährung und Landwirtschaft: Berlin, Germany, 2014.
9. Malyan, S.K.; Bhatia, A.; Fagodiya, R.K.; Kumar, S.S.; Kumar, A.; Gupta, D.K.; Tomer, R.; Harit, R.C.; Kumar, V.; Jain, N.; et al. Plummeting Global Warming Potential by Chemicals Interventions in Irrigated Rice: A Lab to Field Assessment. *Agric. Ecosyst. Environ.* **2021**, *319*, 107545. [CrossRef]
10. Malyan, S.K.; Kumar, S.S.; Fagodiya, R.K.; Ghosh, P.; Kumar, A.; Singh, R.; Singh, L. Biochar for Environmental Sustainability in the Energy-Water-Agroecosystem Nexus. *Renew. Sustain. Energy Rev.* **2021**, *149*, 111379. [CrossRef]
11. Bijay-singh; Ryden, J.C.; Whitchead, D.C. Some Relationships between Denitrification Potential and Fractions of Organic Carbon in Air-Dried and Field-Moist Soils. *Soil Biol. Biochem.* **1988**, *20*, 737–741. [CrossRef]
12. Burford, J.R.; Bremner, J.M. Relationships between the Denitrification Capacities of Soils and Total, Water-Soluble and Readily Decomposable Soil Organic Matter. *Soil Biol. Biochem.* **1975**, *7*, 389–394. [CrossRef]
13. De Catanzaro, J.B.; Beauchamp, E.G. The Effect of Some Carbon Substrates on Denitrification Rates and Carbon Utilization in Soil. *Biol. Fertil. Soils* **1985**, *1*, 183–187. [CrossRef]
14. Gilmour, J.T. The Effects of Soil Properties on Nitrification and Nitrification Inhibition. *Soil Sci. Soc. Am. J.* **1984**, *48*, 1262–1266. [CrossRef]
15. Groffman, P.M.; Butterbach-Bahl, K.; Fulweiler, R.W.; Gold, A.J.; Morse, J.L.; Stander, E.K.; Tague, C.; Tonitto, C.; Vidon, P. Challenges to Incorporating Spatially and Temporally Explicit Phenomena (Hotspots and Hot Moments) in Denitrification Models. *Biogeochemistry* **2009**, *93*, 49–77. [CrossRef]
16. Heinen, M. Simplified Denitrification Models: Overview and Properties. *Geoderma* **2006**, *133*, 444–463. [CrossRef]
17. Malhi, S.S.; McGill, W.B. Nitrification in Three Alberta Soils: Effect of Temperature, Moisture and Substrate Concentration. *Soil Biol. Biochem.* **1982**, *14*, 393–399. [CrossRef]

18. McCarty, G.W.; Bremner, J.M. Factors Affecting the Availability of Organic Carbon for Denitrification of Nitrate in Subsoils. *Biol. Fertil. Soils* **1993**, *15*, 132–136. [CrossRef]
19. Sahrawat, K.L. Factors Affecting Nitrification in Soils. *Commun. Soil Sci. Plant Anal.* **2008**, *39*, 1436–1446. [CrossRef]
20. Peterjohn, W.T. Denitrification: Enzyme Content and Activity in Desert Soils. *Soil Biol. Biochem.* **1991**, *23*, 845–855. [CrossRef]
21. ŠImek, M.; Cooper, J.E. The Influence of Soil PH on Denitrification: Progress towards the Understanding of This Interaction over the Last 50 Years. *Eur. J. Soil Sci.* **2002**, *53*, 345–354. [CrossRef]
22. Šimek, M.; Hopkins, D.W. Regulation of Potential Denitrification by Soil PH in Long-Term Fertilized Arable Soils. *Biol. Fertil. Soils* **1999**, *30*, 41–47. [CrossRef]
23. Rodrigo, A.; Recous, S.; Neel, C.; Mary, B. Modelling Temperature and Moisture Effects on C–N Transformations in Soils: Comparison of Nine Models. *Ecol. Model.* **1997**, *102*, 325–339. [CrossRef]
24. Müller, C.; Clough, T.J. Advances in Understanding Nitrogen Flows and Transformations: Gaps and Research Pathways. *J. Agric. Sci.* **2014**, *152*, 34–44. [CrossRef]
25. Balaine, N.; Clough, T.J.; Beare, M.H.; Thomas, S.M.; Meenken, E.D.; Ross, J.G. Changes in Relative Gas Diffusivity Explain Soil Nitrous Oxide Flux Dynamics. *Soil Sci. Soc. Am. J.* **2013**, *77*, 1496–1505. [CrossRef]
26. Federal Ministry of Justice and Consumer Protection. *Düngeverordnung (DüV) Vom 26. Mai 2017. Verordnung Über dDie Anwendung von Düngemitteln, Bodenhilfsstoffen, Kultursubstraten und Pflanzenhilfsmitteln nach den Grundsätzen der Guten Fachlichen Praxis Beim Düngen*; Bundesanzeiger Verlag GmbH: Köln, Germany, 2017.
27. Deppe, M.; Well, R.; Giesemann, A.; Spott, O.; Flessa, H. Soil $N_2O$ Fluxes and Related Processes in Laboratory Incubations Simulating Ammonium Fertilizer Depots. *Soil Biol. Biochem.* **2017**, *104*, 68–80. [CrossRef]
28. Dörsch, P.; Braker, G.; Bakken, L.R. Community-Specific PH Response of Denitrification: Experiments with Cells Extracted from Organic Soils. *FEMS Microbiol. Ecol.* **2012**, *79*, 530–541. [CrossRef] [PubMed]
29. Petersen, S.O.; Nielsen, T.H.; Frostegård, Å.; Olesen, T. $O_2$ Uptake, C Metabolism and Denitrification Associated with Manure Hot-Spots. *Soil Biol. Biochem.* **1996**, *28*, 341–349. [CrossRef]
30. Markfoged, R.; Nielsen, L.P.; Nyord, T.; Ottosen, L.D.M.; Revsbech, N.P. Transient $N_2O$ Accumulation and Emission Caused by $O_2$ Depletion in Soil after Liquid Manure Injection. *Eur. J. Soil Sci.* **2011**, *62*, 541–550. [CrossRef]
31. Zhu, K.; Bruun, S.; Larsen, M.; Glud, R.N.; Jensen, L.S. Spatial Oxygen Distribution and Nitrous Oxide Emissions from Soil after Manure Application: A Novel Approach Using Planar Optodes. *J. Environ. Qual.* **2014**, *43*, 1809–1812. [CrossRef]
32. Petersen, S.O.; Nissen, H.H.; Lund, I.; Ambus, P. Redistribution of Slurry Components as Influenced by Injection Method, Soil, and Slurry Properties. *J. Environ. Qual.* **2003**, *32*, 2399–2409. [CrossRef]
33. Petersen, S.O.; Baral, K.R.; Arthur, E. Manure Distribution as a Predictor of $N_2O$ Emissions from Soil. *Anim. Prod. Sci.* **2016**, *56*, 549. [CrossRef]
34. SRU. *Stickstoff: Lösungsstrategien für ein Drängendes Umweltproblem. Sondergutachten*; Sachverständigenrat für Umweltfragen (SRU): Berlin, Germany, 2015; Available online: https://www.umweltrat.de/ (accessed on 4 May 2022).
35. Baral, K.R.; Arthur, E.; Olesen, J.E.; Petersen, S.O. Predicting Nitrous Oxide Emissions from Manure Properties and Soil Moisture: An Incubation Experiment. *Soil Biol. Biochem.* **2016**, *97*, 112–120. [CrossRef]
36. John, P.S.; Buresh, R.J.; Prasad, R.; Pandey, R.K. Nitrogen Gas ($N_2$ + $N_2O$) Flux from Urea Applied to Lowland Rice as Affected by Green Manure. *Plant Soil* **1989**, *119*, 7–13. [CrossRef]
37. Zhang, Y.; Wang, R.; Pan, Z.; Liu, Y.; Zheng, X.; Ju, X.; Zhang, C.; Butterbach-Bahl, K.; Huang, B. Fertilizer Nitrogen Loss via $N_2$ Emission from Calcareous Soil Following Basal Urea Application of Winter Wheat. *Atmos. Ocean. Sci. Lett.* **2019**, *12*, 91–97. [CrossRef]
38. Butterbach-Bahl, K.; Baggs, E.M.; Dannenmann, M.; Kiese, R.; Zechmeister-Boltenstern, S. Nitrous Oxide Emissions from Soils: How Well Do We Understand the Processes and Their Controls? *Philos. Trans. R. Soc. B Biol. Sci.* **2013**, *368*, 20130122. [CrossRef] [PubMed]
39. Li, C.; Salas, W.; Zhang, R.; Krauter, C.; Rotz, A.; Mitloehner, F. Manure-DNDC: A Biogeochemical Process Model for Quantifying Greenhouse Gas and Ammonia Emissions from Livestock Manure Systems. *Nutr. Cycl. Agroecosyst.* **2012**, *93*, 163–200. [CrossRef]
40. Sommer, S.G.; Petersen, S.O.; Møller, H.B. Algorithms for Calculating Methane and Nitrous Oxide Emissions from Manure Management. *Nutr. Cycl. Agroecosyst.* **2004**, *69*, 143–154. [CrossRef]
41. Probert, M.E. The APSIM Manure Model: Improvements in Predictability and Application to Laboratory Studies. *Model. Nutr. Manag. Trop. Crop. Syst.* **2004**, *114*, 76–84.
42. IUSS Working Group WRB. *World Reference Base for Soil Resources 2014, Update 2015 International Soil Classification System for Naming Soils and Creating Legends for Soil Maps*; World Soil Resources Reports No. 106; FAO: Rome, Italy, 2015.
43. Böttcher, J.; Springob, G.; Duijnisveld, W.H.M. Sandige Böden Und Deren Wasser- Und Stoffhaushalt Unter Acker Und Nadelwald Im Fuhrherger Feld. *Mitt. Dtsch. Bodenkd. Ges. Exkurs.* **1999**, *90*, 405–425.
44. Well, R.; Höper, H.; Mehranfar, O.; Meyer, K. Denitrification in the Saturated Zone of Hydromorphic Soils—Laboratory Measurement, Regulating Factors and Stochastic Modeling. *Soil Biol. Biochem.* **2005**, *37*, 1822–1836. [CrossRef]
45. Lewicka-Szczebak, D.; Augustin, J.; Giesemann, A.; Well, R. Quantifying $N_2O$ Reduction to $N_2$ Based on $N_2O$ Isotopocules—Validation with Independent Methods (Helium Incubation and $^{15}N$ Gas Flux Method). *Biogeosciences* **2017**, *14*, 711–732. [CrossRef]
46. Hantschel, R.E.; Flessa, H.; Beese, F. An Automated Microcosm System for Studying Soil Ecological Processes. *Soil Sci. Soc. Am. J.* **1994**, *58*, 401–404. [CrossRef]

47. Säurich, A.; Tiemeyer, B.; Dettmann, U.; Don, A. How Do Sand Addition, Soil Moisture and Nutrient Status Influence Greenhouse Gas Fluxes from Drained Organic Soils? *Soil Biol. Biochem.* **2019**, *135*, 71–84. [CrossRef]
48. Spott, O.; Russow, R.; Apelt, B.; Stange, C.F. A $^{15}$N-Aided Artificial Atmosphere Gas Flow Technique for Online Determination of Soil $N_2$ Release Using the Zeolite Köstrolith SX6®. *Rapid Commun. Mass Spectrom.* **2006**, *20*, 3267–3274. [CrossRef] [PubMed]
49. Kemmann, B.; Wöhl, L.; Fuß, R.; Schrader, S.; Well, R.; Ruf, T. $N_2$ and $N_2O$ Mitigation Potential of Replacing Maize with the Perennial Biomass Crop *Silphium Perfoliatum*—An Incubation Study. *GCB Bioenergy* **2021**, *13*, 1649–1665. [CrossRef]
50. Well, R.; Kurganova, I.; Lopesdegerenyu, V.; Flessa, H. Isotopomer Signatures of Soil-Emitted $N_2O$ under Different Moisture Conditions—A Microcosm Study with Arable Loess Soil. *Soil Biol. Biochem.* **2006**, *38*, 2923–2933. [CrossRef]
51. Lewicka-Szczebak, D.; Well, R.; Giesemann, A.; Rohe, L.; Wolf, U. An Enhanced Technique for Automated Determination of $^{15}$N Signatures of $N_2$, ($N_2$ + $N_2O$) and $N_2O$ in Gas Samples. *Rapid Commun. Mass Spectrom.* **2013**, *27*, 1548–1558. [CrossRef]
52. Kool, D.M.; Hoffland, E.; Abrahamse, S.; van Groenigen, J.W. What Artificial Urine Composition Is Adequate for Simulating Soil $N_2O$ Fluxes and Mineral N Dynamics? *Soil Biol. Biochem.* **2006**, *38*, 1757–1763. [CrossRef]
53. Kalbitz, K.; Schmerwitz, J.; Schwesig, D.; Matzner, E. Biodegradation of Soil-Derived Dissolved Organic Matter as Related to Its Properties. *Geoderma* **2003**, *113*, 273–291. [CrossRef]
54. Davidson, E.A.; Hart, S.C.; Shanks, C.A.; Firestone, M.K. Measuring Gross Nitrogen Mineralization, and Nitrification by 15 N Isotopic Pool Dilution in Intact Soil Cores. *J. Soil Sci.* **1991**, *42*, 335–349. [CrossRef]
55. Dyckmans, J.; Eschenbach, W.; Langel, R.; Szwec, L.; Well, R. Nitrogen Isotope Analysis of Aqueous Ammonium and Nitrate by Membrane Inlet Isotope Ratio Mass Spectrometry (MIRMS) at Natural Abundance Levels. *Rapid Commun. Mass Spectrom.* **2021**, *35*, e9077. [CrossRef]
56. Moldrup, P.; Chamindu Deepagoda, T.K.K.; Hamamoto, S.; Komatsu, T.; Kawamoto, K.; Rolston, D.E.; Jonge, L.W. Structure-Dependent Water-Induced Linear Reduction Model for Predicting Gas Diffusivity and Tortuosity in Repacked and Intact Soil. *Vadose Zone J.* **2013**, *12*, 1–11. [CrossRef]
57. Van Rossum, G.; Drake, F.L. *Python 3 Reference Manual*; CreateSpace: Scotts Valley, CA, USA, 2009; ISBN 1-4414-1269-7.
58. R Core Team. *R: A Language and Environment for Statistical Computing*; R Core Team: Vienna, Austria, 2020.
59. Kutilek, M.; Nielsen, D. *Soil Hydrology. Textbook for Students of Soil Science, Agriculture, Forestry, Geoecology, Hydrology, Geomorphology and Other Related Disciplines*; Cremlingen-Destedt: Freising, Germany, 1994.
60. Robertson, G.P.; Groffman, P.M. Nitrogen Transformations. *Soil Microbiol. Ecol. Biochem.* **2015**, 421–446. [CrossRef]
61. Norton, J.; Ouyang, Y. Controls and Adaptive Management of Nitrification in Agricultural Soils. *Front. Microbiol.* **2019**, *10*. [CrossRef] [PubMed]
62. Parton, W.J.; Holland, E.A.; Del Grosso, S.J.; Hartman, M.D.; Martin, R.E.; Mosier, A.R.; Ojima, D.S.; Schimel, D.S. Generalized Model for $NO_x$ and $N_2O$ Emissions from Soils. *J. Geophys. Res. Atmos.* **2001**, *106*, 17403–17419. [CrossRef]
63. Petersen, S.O.; Ambus, P.; Elsgaard, L.; Schjønning, P.; Olesen, J.E. Long-Term Effects of Cropping System on $N_2O$ Emission Potential. *Soil Biol. Biochem.* **2013**, *57*, 706–712. [CrossRef]
64. Paul, J.W.; Beauchamp, E.G. Effect of Carbon Constituents in Manure on Denitrification in Soil. *Can. J. Soil Sci.* **1989**, *69*, 49–61. [CrossRef]
65. Schimel, D.S. Calculation of Microbial Growth Eftkiency from $^{15}$N Immobilization. *Biogeochemistry* **1988**, *6*, 239–243. [CrossRef]
66. Hardison, A.K.; Algar, C.K.; Giblin, A.E.; Rich, J.J. Influence of Organic Carbon and Nitrate Loading on Partitioning between Dissimilatory Nitrate Reduction to Ammonium (DNRA) and N2 Production. *Geochim. Cosmochim. Acta* **2015**, *164*, 146–160. [CrossRef]
67. Friedl, J.; De Rosa, D.; Rowlings, D.W.; Grace, P.R.; Müller, C.; Scheer, C. Dissimilatory Nitrate Reduction to Ammonium (DNRA), Not Denitrification Dominates Nitrate Reduction in Subtropical Pasture Soils upon Rewetting. *Soil Biol. Biochem.* **2018**, *125*, 340–349. [CrossRef]
68. Skaggs, T.H.; Leij, F.J. 6.3 Solute Transport: Theoretical Background. *Methods Soil Anal.* **2002**, *5*, 1353–1380. [CrossRef]
69. Phan, N.-T.; Kim, K.-H.; Parker, D.; Jeon, E.-C.; Sa, J.-H.; Cho, C.-S. Effect of Beef Cattle Manure Application Rate on $CH_4$ and $CO_2$ Emissions. *Atmos. Environ.* **2012**, *63*, 327–336. [CrossRef]
70. Chantigny, M.H.; Rochette, P.; Angers, D.A. Short-Term C and N Dynamics in a Soil Amended with Pig Slurry and Barley Straw: A Field Experiment. *Can. J. Soil Sci.* **2001**, *81*, 131–137. [CrossRef]
71. Li, Y.; Clough, T.J.; Moinet, G.Y.K.; Whitehead, D. Emissions of Nitrous Oxide, Dinitrogen and Carbon Dioxide from Three Soils Amended with Carbon Substrates under Varying Soil Matric Potentials. *Eur. J. Soil Sci.* **2021**, *72*, 2261–2275. [CrossRef]
72. Duncan, E.W.; Dell, C.J.; Kleinman, P.J.A.; Beegle, D.B. Nitrous Oxide and Ammonia Emissions from Injected and Broadcast-Applied Dairy Slurry. *J. Environ. Qual.* **2017**, *46*, 36–44. [CrossRef] [PubMed]
73. Philippot, L.; Hallin, S.; Schloter, M. Ecology of Denitrifying Prokaryotes in Agricultural Soil. *Adv. Agron.* **2007**, *96*, 249–305. [CrossRef]
74. Schjønning, P.; Thomsen, I.K.; Moldrup, P.; Christensen, B.T. Linking Soil Microbial Activity to Water- and Air-Phase Contents and Diffusivities. *Soil Sci. Soc. Am. J.* **2003**, *67*, 156–165. [CrossRef]
75. Stepniewski, W. Oxygen-Diffusion and Strength as Related to Soil Compaction. I. ODR. *Pol. J. Soil Sci.* **1980**, *13*, 3–13.
76. Grundmann, G.L.; Rolston, D.E. Water Function Approximation to Degree of Anaerobiosis Associated with Denitrification. *Soil Sci.* **1987**, *144*, 437–441. [CrossRef]

77. Groffman, P.M.; Tiedje, J.M. Denitrification Hysteresis During Wetting and Drying Cycles in Soil. *Soil Sci. Soc. Am. J.* **1988**, *52*, 1626–1629. [CrossRef]
78. Čuhel, J.; Šimek, M.; Laughlin, R.J.; Bru, D.; Chèneby, D.; Watson, C.J.; Philippot, L. Insights into the Effect of Soil PH on $N_2O$ and $N_2$ Emissions and Denitrifier Community Size and Activity. *Appl. Environ. Microbiol.* **2010**, *76*, 1870–1878. [CrossRef]
79. Senbayram, M.; Well, R.; Bol, R.; Chadwick, D.R.; Jones, D.L.; Wu, D. Interaction of Straw Amendment and Soil $NO_3^-$ Content Controls Fungal Denitrification and Denitrification Product Stoichiometry in a Sandy Soil. *Soil Biol. Biochem.* **2018**, *126*, 204–212. [CrossRef]
80. Bergaust, L.; Mao, Y.; Bakken, L.R.; Frostegård, Å. Denitrification Response Patterns during the Transition to Anoxic Respiration and Posttranscriptional Effects of Suboptimal Ph on Nitrogen Oxide Reductase in Paracoccus Denitrificans. *Appl. Environ. Microbiol.* **2010**, *76*, 6387–6396. [CrossRef] [PubMed]
81. Liu, B.; Mørkved, P.T.; Frostegård, Å.; Bakken, L.R. Denitrification Gene Pools, Transcription and Kinetics of NO, N2O and N2 Production as Affected by Soil PH. *FEMS Microbiol. Ecol.* **2010**, *72*, 407–417. [CrossRef] [PubMed]
82. Liu, B.; Frostegård, Å.; Bakken, L.R. Impaired Reduction of $N_2O$ to $N_2$ in Acid Soils Is Due to a Posttranscriptional Interference with the Expression of NosZ. *mBio* **2014**, *5*, e01383-14. [CrossRef] [PubMed]
83. Frostegård, Å.; Vick, S.H.W.; Lim, N.Y.N.; Bakken, L.R.; Shapleigh, J.P. Linking Meta-Omics to the Kinetics of Denitrification Intermediates Reveals PH-Dependent Causes of $N_2O$ Emissions and Nitrite Accumulation in Soil. *ISME J.* **2021**, *16*, 26–37. [CrossRef]
84. Köster, J.R.; Cárdenas, L.; Senbayram, M.; Bol, R.; Well, R.; Butler, M.; Mühling, K.H.; Dittert, K. Rapid Shift from Denitrification to Nitrification in Soil after Biogas Residue Application as Indicated by Nitrous Oxide Isotopomers. *Soil Biol. Biochem.* **2011**, *43*, 1671–1677. [CrossRef]
85. Wrage-Mönnig, N.; Horn, M.A.; Well, R.; Müller, C.; Velthof, G.; Oenema, O. The Role of Nitrifier Denitrification in the Production of Nitrous Oxide Revisited. *Soil Biol. Biochem.* **2018**, *123*, A3–A16. [CrossRef]
86. Hink, L.; Nicol, G.W.; Prosser, J.I. Archaea Produce Lower Yields of $N_2O$ than Bacteria during Aerobic Ammonia Oxidation in Soil. *Environ. Microbiol.* **2017**, *19*, 4829–4837. [CrossRef]
87. Petersen, S.O.; Andersen, M.N. Influence of Soil Water Potential and Slurry Type on Denitrification Activity. *Soil Biol. Biochem.* **1996**, *28*, 977–980. [CrossRef]
88. Frostegård, A.; Petersen, S.O.; Bååth, E.; Nielsen, T.H. Dynamics of a Microbial Community Associated with Manure Hot Spots as Revealed by Phospholipid Fatty Acid Analyses. *Appl. Environ. Microbiol.* **1997**, *63*, 2224–2231. [CrossRef]
89. Nielsen, T.H.; Nielsen, L.P.; Revsbech, N.P. Nitrification and Coupled Nitrification-Denitrification Associated with a Soil-Manure Interface. *Soil Sci. Soc. Am. J.* **1996**, *60*, 1829–1840. [CrossRef]
90. Scholefield, D.; Hawkins, J.M.B.; Jackson, S.M. Use of a Flowing Helium Atmosphere Incubation Technique to Measure the Effects of Denitrification Controls Applied to Intact Cores of a Clay Soil. *Soil Biol. Biochem.* **1997**, *29*, 1337–1344. [CrossRef]
91. Müller, C.; Laughlin, R.J.; Spott, O.; Rütting, T. Quantification of $N_2O$ Emission Pathways via a $^{15}N$ Tracing Model. *Soil Biol. Biochem.* **2014**, *72*, 44–54. [CrossRef]
92. Rohe, L.; Apelt, B.; Vogel, H.-J.; Well, R.; Wu, G.-M.; Schlüter, S. Denitrification in Soil as a Function of Oxygen Availability at the Microscale. *Biogeosciences* **2021**, *18*, 1185–1201. [CrossRef]
93. Schlüter, S.; Henjes, S.; Zawallich, J.; Bergaust, L.; Horn, M.; Ippisch, O.; Vogel, H.-J.; Dörsch, P. Denitrification in Soil Aggregate Analogues-Effect of Aggregate Size and Oxygen Diffusion. *Front. Environ. Sci.* **2018**, *6*, 17. [CrossRef]
94. Buchen, C.; Lewicka-Szczebak, D.; Fuß, R.; Helfrich, M.; Flessa, H.; Well, R. Fluxes of $N_2$ and $N_2O$ and Contributing Processes in Summer after Grassland Renewal and Grassland Conversion to Maize Cropping on a Plaggic Anthrosol and a Histic Gleysol. *Soil Biol. Biochem.* **2016**, *101*, 6–19. [CrossRef]
95. Lewicka-Szczebak, D.; Well, R. The $^{15}N$ Gas-Flux Method to Determine $N_2$ Flux: A Comparison of Different Tracer Addition Approaches. *Soil* **2020**, *6*, 145–152. [CrossRef]
96. Rummel, P.S.; Pfeiffer, B.; Pausc, J.; Well, R.; Schneider, D.; Dittert, K. Maize Root and Shoot Litter Quality Controls Short-Term $CO_2$ and $N_2O$ Emissions and Bacterial Community Structure of Arable Soil. *Biogeosciences* **2020**, *17*, 1181–1198. [CrossRef]